Asymptotic scaling from strong coupling

Massimo Campostrini, Paolo Rossi, and Ettore Vicari
Dipartimento di Fisica dell'Università and INFN, I-56126 Pisa, Italy
(Received 7 September 1994)

Strong-coupling analysis of two-dimensional chiral models, extended to fifteenth order, allows for the identification of a scaling region where known continuum results are reproduced with great accuracy, and asymptotic scaling predictions are satisfied. The properties of the large-N second-order phase transition are quantitatively investigated.

Two-dimensional principal chiral models can be considered as a theoretical physics laboratory in that these models display a rich physical structure and share with four-dimensional gauge theories a number of fundamental properties: non-Abelian symmetry with fields in the matrix representation, asymptotic freedom, and a large-N limit which is represented by a sum over planar diagrams. However, the absence of local gauge invariance and the reduced number of dimensions make chiral models much simpler to handle both by analytical and by numerical methods. We can therefore try to make progress in techniques suitable for four-dimensional (4D) gauge theories by testing them first on 2D chiral models.

Recent developments in the analytical and numerical study of lattice two-dimensional $SU(N) \times SU(N)$ principal chiral models have shown the existence of a scaling region, where continuum predictions for dimensionless ratios of physical quantities are substantially verified [1].

The scaling region begins at very small values of the correlation length, $\xi \gtrsim 2$, well within the region of convergence of the strong-coupling series. Moreover by performing a nonperturbative change of variables [2] from the standard Lagrangian (inverse) coupling β to

$$\beta_E = \frac{N^2-1}{8N^2E},\tag{1}$$

where E is the internal energy of the system (which can be measured in a Monte Carlo simulation), one can find agreement in the whole scaling region between the measured mass scale and the prediction for the mass gap/Λ parameter ratio offered by the two-loop continuum renormalization group supplemented by a Bethe ansatz evaluation [3]. As a matter of fact, this may be thought of as evidence for asymptotic scaling within the strong-coupling regime.

We therefore felt motivated for a significant effort in improving our analytical knowledge of the strong-coupling series for principal chiral models, in order to check the accuracy of predictions for physical (continuum) quantities solely based on strong-coupling computations.

As a by-product, strong-coupling series can be analyzed to investigate the critical behavior of the $N = \infty$ theory, where Monte Carlo data seem to indicate the existence of a transition at finite β.

Strong-coupling calculations for matrix models are best performed by means of the character expansion. Even the

character expansion, however, eventually runs into almost intractable technical difficulties, related to two concurrent phenomena: (1) the proliferation of configurations contributing to large orders of the series, whose number essentially grows like that of nonbacktracking random walks; (2) the appearance of topologically nontrivial configurations corresponding to group integrations that cannot be performed by applying the orthogonality of characters and the decomposition of their products into sums.

We shall devote an extended paper to a complete presentation of our fifteenth-order strong-coupling character expansions for arbitrary $U(N)$ groups [extension to $SU(N)$ is then obtained by the techniques discussed in Refs. [4] and [1]]. We only mention that we had to rely on a mixed approach: problem (1) above was tackled by a computer program generating all nonbacktracking random walks, computing their correct multiplicities, and classifying them according to their topology; problem (2), requiring the analytical evaluation of many classes of nontrivial group integrals, and extraction of their connected contribution to the relevant physical quantities, was solved by more conventional algebraic techniques.

We pushed our computational techniques close to their limit; in order to extend our results to higher orders, a more algorithmic approach would be in order, especially for recognition of diagram topologies and group integration.

In the present Rapid Communication we shall only exhibit the results we obtained by taking the large-N limit of all the quantities we computed. In the strong-coupling domain, convergence to $N = \infty$ is usually fast, and therefore large-N results are a good illustration of a phenomenology that repeats itself (with small corrections) for finite values of N.

Starting from the standard nearest-neighbor interaction

$$S_L = -2N\beta \sum_{x,\mu} \text{ReTr}\{U(x)\,U^\dagger(x+\mu)\},\tag{2}$$

we computed the large-N free energy

$$F = \frac{1}{N^2}\ln \int dU_n \exp(-S_L)\tag{3}$$

to eighteenth order in the expansion in powers of β. The resulting series is

$$F = 2\beta^2 + 2\beta^4 + 4\beta^6 + 19\beta^8 + 96\beta^{10} + 604\beta^{12} + 4036\beta^{14}$$
$$+ \frac{58471}{2}\beta^{16} + \frac{663184}{3}\beta^{18} + O(\beta^{20}). \tag{4}$$

The two-point Green's functions, normalized to obtain a finite large-N limit, are

$$G(x) = \frac{1}{N}\text{Tr}\{U^\dagger(x)U(0)\}. \tag{5}$$

We computed all nontrivial two-point Green's functions up to $O(\beta^{15})$. The corresponding information is appropriately summarized by introducing the lattice Fourier transform

$$\tilde{G}(p) = \sum_x G(x)\exp(ip\cdot x) \tag{6}$$

and evaluating the inverse propagator

$$\tilde{G}^{-1}(p) = A_0 + \hat{p}^2 A_1 + [(\hat{p}^2)^2 - \hat{p}^4]A_{2,0} + \hat{p}^4 A_{2,2} + \hat{p}^2[(\hat{p}^2)^2 - \hat{p}^4]A_{3,1} + \hat{p}^6 A_{3,3} + [(\hat{p}^2)^2 - \hat{p}^4]^2 A_{4,0} + \hat{p}^4[(\hat{p}^2)^2 - \hat{p}^4]A_{4,2}$$
$$+ \hat{p}^8 A_{4,4} + \hat{p}^2[(\hat{p}^2)^2 - \hat{p}^4]^2 A_{5,1} + \hat{p}^6[(\hat{p}^2)^2 - \hat{p}^4]A_{5,3} + \cdots, \tag{7}$$

where

$$A_0 = 1 - 4\beta + 4\beta^2 - 4\beta^3 + 12\beta^4 - 28\beta^5 + 52\beta^6 - 132\beta^7 + 324\beta^8 - 908\beta^9 + 2020\beta^{10} - 6284\beta^{11} + 15284\beta^{12} - 48940\beta^{13}$$
$$+ 116612\beta^{14} - 393132\beta^{15} + O(\beta^{16}),$$

$$A_1 = \beta(1 + \beta^2 + 7\beta^4 + 4\beta^5 + 33\beta^6 + 32\beta^7 + 243\beta^8 + 324\beta^9 + 1819\beta^{10} + 2520\beta^{11} + 14859\beta^{12} + 23084\beta^{13} + 123883\beta^{14})$$
$$+ O(\beta^{16}),$$

$$A_{2,0} = -\beta^6(1 + 6\beta^2 + 8\beta^3 + 57\beta^4 + 116\beta^5 + 500\beta^6 + 1152\beta^7 + 5155\beta^8 + 11632\beta^9) + O(\beta^{16}),$$

$$A_{2,2} = -2\beta^8(1 + 2\beta + 12\beta^2 + 35\beta^3 + 121\beta^4 + 408\beta^5 + 1412\beta^6 + 4264\beta^7) + O(\beta^{16}),$$

$$A_{3,1} = \beta^9\left(1 + \frac{29}{2}\beta^2 + 26\beta^3 + 144\beta^4 + 482\beta^5 + 1806\beta^6\right) + O(\beta^{16}),$$

$$A_{3,3} = 2\beta^{11}(1 + 2\beta + 20\beta^2 + 70\beta^3 + 274\beta^4) + O(\beta^{16}),$$

$$A_{4,0} = -\beta^{12}\left(\frac{5}{2} + 37\beta^2 + 84\beta^3\right) + O(\beta^{16}),$$

$$A_{4,2} = -\beta^{12}(1 + 31\beta^2 + 64\beta^3) + O(\beta^{16}),$$

$$A_{4,4} = -2\beta^{14}(1 + 2\beta) + O(\beta^{16}),$$

$$A_{5,1} = 7\beta^{15} + O(\beta^{16}),$$

$$A_{5,3} = \beta^{15} + O(\beta^{16}). \tag{8}$$

A number of physically interesting quantities can be extracted from $\tilde{G}^{-1}(p)$. In particular the magnetic susceptibility is

$$\chi = \sum_x G(x) = \frac{1}{A_0} = 1 + 4\beta + 12\beta^2 + 36\beta^3 + 100\beta^4 + 284\beta^5 + 796\beta^6 + 2276\beta^7 + 6444\beta^8 + 18572\beta^9 + 53292\beta^{10} + 155500\beta^{11}$$
$$+ 451516\beta^{12} + 1330796\beta^{13} + 3904908\beta^{14} + 11617356\beta^{15} + O(\beta^{16}), \tag{9}$$

while the second-moment definition of the correlation length leads to

$$M_G^2 = \frac{1}{\langle x^2 \rangle_G} = \frac{A_0}{A_1} = \frac{1}{\beta} - 4 + 3\beta + 2\beta^3 - 4\beta^4 + 12\beta^5 - 40\beta^6 + 84\beta^7 - 296\beta^8 + 550\beta^9 - 1904\beta^{10} + 3316\beta^{11} - 15248\beta^{12}$$
$$+ 27756\beta^{13} + O(\beta^{14}), \tag{10}$$

and the corresponding wave-function renormalization is $Z_G = A_1^{-1}$.

Moreover, by solving the equation

$$\tilde{G}^{-1}(p_x = i\mu_s, p_y = 0) = 0,\tag{11}$$

we can compute the wall-wall correlation length, i.e., the true mass-gap μ_s; Eq. (11) is algebraic in

$$M_s^2 = 2(\cosh\mu_s - 1) = \frac{1}{\beta} - 4 + 3\beta + 2\beta^3 - 4\beta^4 + 10\beta^5 - 28\beta^6 + 48\beta^7 - 206\beta^8 + 352\beta^9 - 1506\beta^{10} + 2326\beta^{11} + O(\beta^{12}).\tag{12}$$

By solving

$$\tilde{G}^{-1}(p_x = i\mu_d/\sqrt{2}, p_y = i\mu_d/\sqrt{2}) = 0\tag{13}$$

we find the diagonal wall-wall correlation length

$$M_d^2 = 4\left(\cosh\frac{\mu_d}{\sqrt{2}} - 1\right) = \frac{1}{\beta} - 4 + 3\beta + \frac{3}{2}\beta^3 - 3\beta^5 - \frac{169}{8}\beta^7$$
$$- 220\beta^9 + O(\beta^{11}).\tag{14}$$

In order to obtain the highest-order contribution to M_s^2, it was necessary to compute a few (long-distance) Green's functions to sixteenth and seventeenth order.

Lattice chiral models have a peak in the specific heat

$$C = \frac{1}{N}\frac{dE}{dT}, \quad T = \frac{1}{N\beta},\tag{15}$$

which becomes more and more pronounced with increasing N [1]. Figure 1 shows Monte Carlo data for the specific heat of SU(N) models for $N = 21, 30$ and U(N) models for $N = 15, 21$. [We recall that U(N) models at finite N should experience a phase transition with a pattern similar to the XY model, but its location is beyond the specific heat peak.] With increasing N, the positions of the peaks in SU(N) and U(N) seem to approach the same value of β, consistently with the fact that SU(N) and U(N) models must have the same large-N limit. This should be considered an indication of a phase transition at $N = \infty$; a rough extrapolation of the C

data indicates a critical coupling $\beta_c \simeq 0.306$. Extrapolating the values of $\xi_G = 1/M_G$ and β_E at the peak of C to $N = \infty$, we obtain, respectively, $\xi_G^{(c)} \simeq 2.8$ and $\beta_E^{(c)} \simeq 0.220$.

The above picture is confirmed by an analysis of the large-N eighteenth-order strong-coupling series of C, based on the method of the integral approximants [5,6]. We indeed obtained quite stable results showing the critical behavior

$$C \sim |\beta - \beta_c|^{-\alpha},\tag{16}$$

with $\beta_c \cong 0.306$ and $\alpha \cong 0.2$, in agreement with the extrapolation of Monte Carlo data. Figure 1 shows that simulation data of C approach, for growing N, the strong-coupling determination.

In spite of the existence of a phase transition at $N = \infty$, Monte Carlo data show scaling and asymptotic scaling (in the β_E scheme) even for β smaller than the peak of the specific heat, suggesting an effective decoupling of the modes responsible for the phase transition from those determining the physical continuum limit; this phenomenon motivated us to use the strong-coupling approach to test scaling and asymptotic scaling. In Fig. 2 we plot the dimensionless ratio μ_s/M_G vs the correlation length $\xi_G \equiv 1/M_G$, as obtained from our strong-coupling series. Notice the stability of the curve for a large region of values of ξ_G and the good agreement (within about 1%) with the continuum large-N value extrapolated by Monte Carlo data $\mu_s/M_G = 0.991(1)$ [1].

In order to test asymptotic scaling we perform the variable change indicated in Eq. (1), evaluating the energy from its strong-coupling series
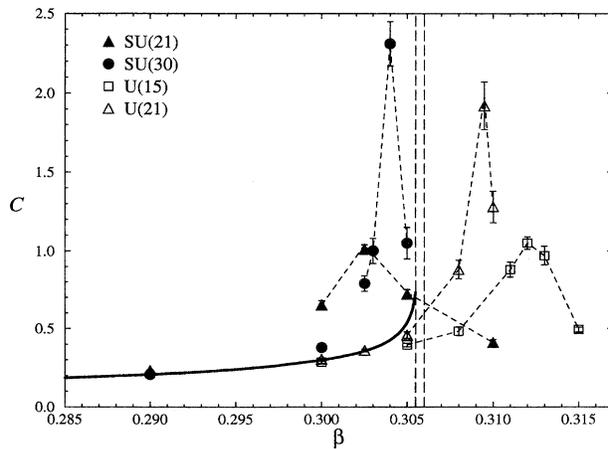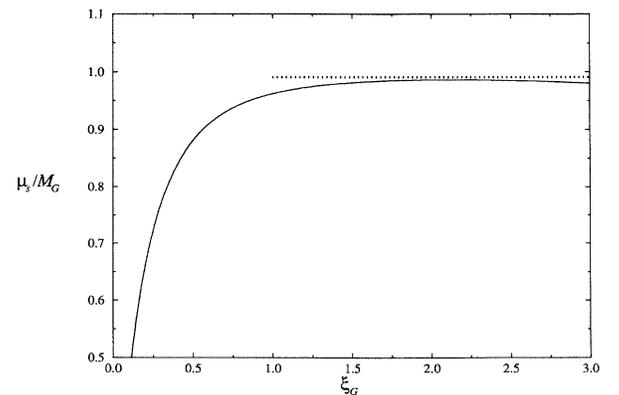

FIG. 1. Specific heat vs β. The solid line represents the resummation of the strong-coupling series, whose estimate of the critical β is indicated by the vertical dashed lines.

FIG. 2. μ_s/M_G vs $\xi_G \equiv 1/M_G$. The dashed line represents the continuum result from Monte Carlo data.
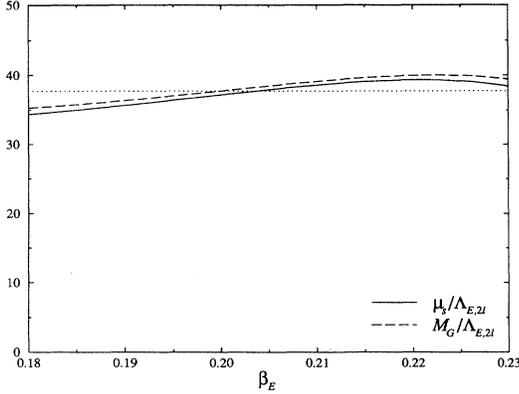
FIG. 3. Asymptotic scaling test by using strong-coupling estimates. The dotted line represents the exact result (18).

$$E = 1 - \frac{1}{4}\frac{\partial F}{\partial \beta} = 1 - G((1,0)) \qquad (17)$$

[cf. Eq. (3)]. The asymptotic scaling formula for the mass gap in the β_E scheme is, in the large-N limit,

$$\mu \cong \sqrt{\frac{\pi}{e}}\, 16\exp\left(\frac{\pi}{4}\right)\Lambda_{E,2l}(\beta_E),$$

$$\Lambda_{E,2l}(\beta_E) = \sqrt{8\pi\beta_E}\exp(-8\pi\beta_E); \qquad (18)$$

β_E can be expressed as a strong-coupling expanded function of β by means of Eq. (17). In Fig. 3 the strong-coupling estimates of $\mu_s/\Lambda_{E,2l}$ and $M_G/\Lambda_{E,2l}$ are plotted vs β_E, for a region of coupling corresponding to correlation lengths $1 \lesssim \xi_G \lesssim 3$. These quantities agree with the exact continuum prediction within 5% in the whole region.

Since the large-N β function in the β_E scheme is not singular (as shown by Monte Carlo data [1] and strong-coupling analysis) and the specific heat has a divergence at β_c, then the relationship

$$\beta_E(T_E) = \frac{8N^2}{N^2-1}C(T)\beta_L(T) \qquad (19)$$

between the β function in the standard scheme $\beta_L(T)$ and in the β_E scheme $\beta_E(T_E)$ leads to a nonanalytical zero of $\beta_L(T)$ at β_c: $\beta_L(T) \sim |\beta - \beta_c|^\alpha$, explaining the observed behavior in β of the Monte Carlo data for the mass gap at large N [1].

This phenomenon is further confirmed by an analysis of the strong-coupling series of χ and M_G^2. Assuming they are well-behaved functions of the energy, we should have

$$\frac{d\ln\chi}{d\beta} \sim \frac{d\ln M_G^2}{d\beta} \sim |\beta - \beta_c|^{-\alpha}. \qquad (20)$$

Analyzing the corresponding series by a modified integral approximant scheme which forces the approximant to have a singularity at $\beta \approx 0.306$, we found a critical behavior consistent with Eq. (20) ($\alpha \approx 0.2$).

[1] P. Rossi and E. Vicari, Phys. Rev. D **49**, 6072 (1994).
[2] G. Parisi, in *High Energy Physics 1980*, Proceedings of the XXth Conference on High Energy Physics, Madison, Wisconsin, 1980, edited by L. Durand and L. G. Pondrom, AIP Conf. Proc. No. 68 (AIP, New York, 1981).
[3] J. Balog, S. Naik, F. Niedermayer, and P. Weisz, Phys. Rev. Lett. **69**, 873 (1992).
[4] F. Green and S. Samuel, Nucl. Phys. **B190**, 113 (1981).
[5] D. L. Hunter and G. A. Baker, Jr., Phys. Rev. B **19**, 3808 (1979).
[6] M. E. Fisher and H. Au-Yang, J. Phys. A **12**, 1677 (1979).